Control of Three-Dimensional Refractive Indices of Uniaxially-Stretched Cellulose Triacetate with Low-Molecular-Weight Compounds

Kultida Songsurang[1,2], Hikaru Shimada[1], Shogo Nobukawa[1], Masayuki Yamaguchi[1*]

[1]School of Materials Science, Japan Advanced Institute of Science and Technology, 1-1 Asahidai, Nomi, Ishikawa, 923-1292, Japan

[2]Program in Petrochemistry, Faculty of Science, Chulalongkorn University, 254 Phayathai Road, Pathumwan, Bangkok, 10330, Thailand

***Corresponding Author**
M. Yamaguchi
Phone +81-761-51-1621
Fax +81-761-51-1621
e-mail m_yama@jaist.ac.jp

Abstract

A method to control the 3D refractive indices and wavelength dispersion of birefringence of polymer films by uniaxial stretching with addition of various low-molecular-weight compounds (LMCs) with strong polarizability anisotropy is developed. Biomass-derived cellulose triacetate (CTA) films containing a small amount of crystallites at the stretching temperature are found to show planar deformation to some degree only by uniaxial stretching. Although molecular orientation evaluated from the in-plane and out-of-plane birefringences of pure CTA seems consistent with uniaxial deformation, LMC addition pronounces the deviation of the refractive index from uniaxial symmetry. Rod-shaped molecules are found to greatly enhance both in-plane and out-of-plane birefringences because of their marked orientation in the stretching direction. Conversely, the out-of-plane birefringence increases more than the in-plane one upon addition of disk-shaped molecules, because the LMC molecules tend to be embedded in the film plane. Consequently, 3D refractive indices of CTA can be controlled only by uniaxial stretching, not biaxial one, with an aid of an anisotropic LMC.

Keywords: Birefringence; Cellulose triacetate; Blend; Orientation

1. Introduction

Cellulose triacetate (CTA) is a biomass-derived material that has found application in films produced by solution casting because of its severe thermal degradation beyond its melting point [1-3]. The common optical film applications of CTA include as a photographic film base and polarizer protection film because of the attractive properties of these films such as high transparency and excellent heat resistance [1,3,4]. CTA films are currently widely employed in liquid crystal displays, and show promise for use in advanced systems such as 3D and electroluminescent displays. To be used in polarizer protective and retardation films, it is important to control the birefringence of CTA. For example, polarizer protective films need to be free from birefringence, and thus advanced methods to erase birefringence have been proposed recently [5-7]. For retardation films, specific retardation, *i.e.*, the product of birefringence and thickness, is required.

It is well known that the orientation birefringence of polymers is determined by the chain orientation and polarizability anisotropy of the repeating unit. For example, a polymer showing positive birefringence has a larger molecular polarizability, and thus refractive index, in the main chain direction than those in the perpendicular directions. The magnitude of birefringence is further controlled by the chain orientation in the stretched film. In general, refractive indices in the in-plane directions (n_x and n_y) can be controlled by uniaxial stretching. However, the refractive index in the film-thickness direction (n_z) should be modulated in addition to n_x and n_y to obtain optical displays with a wide viewing angle. Therefore, an advanced method should be used to control the refractive index n_z and to satisfy the relationship between the refractive index in each direction.

To date, the most conventional method to obtain the 3D control of refractive indices is biaxial stretching, as exemplified by van Horn and Winter [8], which has the drawback of

being expensive. Therefore, much attention has been focused on a new alternative method. The Cakmak research group recently reported the thickness distribution of optical anisotropy in solution-cast films in detail, indicating that the refractive index in the film thickness direction can be controlled by solvent evaporation rate [9-11].

As well as 3D control, the wavelength dispersion of birefringence also has to be precisely modulated for high-performance retardation films. For example, a specific retardation, *e.g.*, a quarter or half of the wavelength, should be provided in the whole visible light region for multi-band wave plates. Because most conventional polymers show ordinary wavelength dispersion of orientation birefringence as expressed by the Sellmeier relation (equation 1), various techniques have been proposed to obtain films showing extraordinary dispersion [12-16].

$$\Delta n(\lambda) = A + \frac{B}{\lambda^2 - {\lambda_{ab}}^2}, \quad (1)$$

where λ_{ab} is the wavelength of a vibrational absorption peak in the ultraviolet region, and A and B are the Sellmeier coefficients. We previously found that transparent films of cellulose acetate propionate show positive in-plane birefringence that increases with wavelength; *i.e.*, extraordinary wavelength dispersion [15-17].

Several methods have been already proposed to control the birefringence in polymeric materials, such as copolymerization with appropriate monomers [18], doping with anisotropic crystals [19] and blending with another polymer [14-16] or a low-molecular-weight compound (LMC) [17,20]. In the polymer blend method, miscible polymer pairs showing different signs of intrinsic birefringence with different wavelength dispersion are mixed on a molecular scale to minimize light scattering.

CTA films prepared by solution casting show uniform thickness, high transparency, and adequate mechanical properties. The sign of out-of-plane birefringence in a solution-cast CTA film is opposite to that of the in-plane orientation birefringence in a hot-stretched one. Moreover, the wavelength dispersion of the out-of-plane birefringence is extraordinary for a solution-cast film. Our previous study also revealed that the out-of-plane birefringence and its wavelength dispersion of a solution-cast film can be modified by the addition of an LMC that is miscible with CTA, such as tricresyl phosphate (TCP) [21]. This is attributed to the molecular orientation of TCP induced by the nematic interaction, *i.e.*, intermolecular orientation correlation, between CTA and TCP.

In this study, both the 3D refractive indices and wavelength dispersion of birefringence of films are controlled by uniaxial stretching, in which the anisotropy in the shrinkage between lateral and thickness directions is used. It is well known that the lateral shrinkage of a polymer film extruded from T-die, known as “neck-in”, is small for a polymer melt showing marked strain-hardening in elongational viscosity [22-25]. In other words, the transversal orientation in the film plane occurs to some degree, although it is not so obvious compared with equi-biaxial elongation for a polymer melt with marked strain-hardening. Therefore, long-chain branched polymers, *e.g.*, low-density polyethylene produced by radical polymerization, are preferably used in industry to reduce the neck-in level during T-die film processing. Moreover, various methods to enhance strain-hardening have also been proposed [26-29]. Yamane et al. showed marked strain-hardening in elongational viscosity for poly(lactic acid) (PLA) having a small amount of stereocomplex crystals whose melting point is higher than that of a conventional PLA [27]. Because CTA also contains a small amount of crystallites [1,3], which act as branch points, at the stretching temperature, it is expected to show strain-hardening; *i.e.*, transversal orientation besides the orientation to the stretching

direction, only by uniaxial stretching. The transversal refractive index caused by the transversal orientation of CTA chains is magnified by LMCs because of their nematic interaction with CTA. In this work, two types of LMCs are used from the viewpoint of molecular shape: TCP and triphenyl phosphate (TPP) as disk-shaped molecules and 4-cyano-4'-pentylbiphenyl (5CB) as a rod-shaped one. Finally, the mechanism of this phenomenon is discussed based on molecular orientation. Since the control of 3D refractive indices and their wavelength dispersion are strongly required to produce advanced displays, the phenomenon described in this paper will be seriously considered for the industrial application.

2. Experimental

The polymeric material used in this study was commercially available CTA produced by Acros Organics. The degree of substitution of CTA was 2.96, and its weight-average molecular weight M_w was 3.50×10^5 Dalton, which was evaluated using a gel permeation chromatograph (Tosoh, HLC-8020) with TSK-GEL® GMHXL as a polystyrene standard. TCP and TPP purchased from Daihachi Chemical Industry were employed as disk-shaped LMCs. 5CB from Wako Pure Chemical Industries was used as a rod-shaped LMC. Their chemical structure is shown in Figure 1.

[Fig.1]

CTA films were prepared by solution casting. CTA with/without an LMC (5 wt%) was dissolved in a mixture of dichloromethane (CH_2Cl_2) and methanol (CH_3OH) with a weight ratio of 9 to 1, and stirred for 24 h at room temperature before casting. All samples were perfectly dissolved into the mixed solvent. The resulting solution containing 4 wt% CTA was poured into a flat-bottomed glass petri dish with a diameter of 80 mm and height of

15 mm at room temperature to allow the solvent to evaporate at a uniform rate. The thickness of the films was 100 μm.

Uniaxially oriented films were prepared by hot stretching using a tensile machine with a temperature controller (UBM, DVE-3 S1000) at a draw ratio of 1.5. The stretching temperature was determined from dynamic mechanical analysis (DMA) data with a tensile storage modulus of 10 MPa at 10 Hz. The initial distance between the clamps was 10 mm, and the width of the sample was 5 mm. Because the stretching rate was 0.5 mm s^{-1}, the initial strain rate was 0.05 s^{-1}. The samples were quenched immediately after stretching under a flow of cold air to prevent relaxation of the molecular orientation.

The temperature dependence of oscillatory tensile moduli in the solid state was measured at 10 Hz from 0 to 250 °C at a heating rate of 2 °C min^{-1} by DMA (UBM, E-4000) using rectangular samples that were 5 mm wide and 20 mm long.

The optical properties of the film samples were measured at room temperature by an optical birefringence analyzer (Oji Scientific Instruments, KOBRA-WPR). The retardation in the thickness direction (out-of-plane retardation) R_{th} was determined by retardation measurements at oblique incidence angles of 0° and 40° as a function of wavelength by changing color filters. The corresponding birefringence was calculated using the film thickness measured by a digital micrometer. Prior to measurements, the samples were placed in a chamber (Yamato, IG420) with temperature and humidity controlled at 25 °C and 50% RH, respectively, for 1 day, to control the moisture content in the films. The in-plane retardation (R_{in}) and R_{th} are respectively defined as follows:

$$R_{in} = \Delta n_{in} \times d = \left(n_x - n_y\right) \times d \qquad (2)$$

$$R_{th} = \Delta n_{th} \times d = \left(\frac{n_x + n_y}{2} - n_z \right) \times d \quad (3)$$

where d is film thickness, x is the stretching direction, y is the direction perpendicular to the stretching direction in the film plane, and z is the thickness direction. The refractive indices in the three principal axes, n_x, n_y and n_z, were determined from Δn_{in} and Δn_{th}, assuming the average refractive index $\bar{n}$ is constant irrespective of the stretching procedure. The average refractive index $\bar{n}$ was measured by an Abbe refractometer.

Wide-angle X-ray diffraction (WAXD) patterns were measured using a graphite-monochromatized Cu Kα radiation beam (Rigaku, R-AXIS IIc). The sample film was mounted to direct the X-ray beam in the normal direction of the film.

Attenuated total reflection (ATR) was measured using an infrared absorption spectrometer (Perkin Elmer, Spectrum 100) to study the molecular orientation in the films. KRS-5 was used as an ATR crystal.

Thermal analysis was conducted with a differential scanning calorimeter (Mettler-Toledo, DSC822) under a nitrogen atmosphere. Samples (~10 mg) were heated from room temperature to 320 °C at a heating rate of 20 °C min^{-1}.

3. Results and Discussion

3.1. Characteristics of Solution-Cast Films

The temperature dependence of oscillatory tensile moduli such as storage modulus E' and loss tangent $tan\ \delta$ for CTA and its blends was measured at 10 Hz to determine the temperature at hot stretching. Figure 2 reveals that the glass transition temperature T_g, which

is defined as the peak temperature of *tan δ* in this study, is located around at 209 °C for pure CTA. For the blends, T_g decreases to 180, 179 and 183 °C upon addition of 5 wt% TCP, TPP and 5CB, respectively. The relaxation peaks ascribed to T_g are broad for the blends, which is typical for plasticized polymers. The dynamic mechanical properties of CTA/TCP and CTA/TPP are similar, while CTA/5CB shows a slightly higher T_g with a broader peak than the other blends. Furthermore, E' shows a plateau beyond the glass-to-rubber transition, which is much higher than the rubbery plateau modulus for a typical polymer [30]. This is attributed to the presence of CTA crystallites. DSC measurements indicate that the melting point T_m of CTA is around 303 °C, which is higher than the stretching temperature. Therefore, the crystallites act as crosslinking or branching points during hot stretching.

[Fig.2]

The wavelength dispersion of the out-of-plane birefringence of the solution-cast films is shown in Figure 3. CTA shows positive birefringence ($n_z<n_x$, n_y) that increases with wavelength; *i.e.*, extraordinary wavelength dispersion. Because the birefringence of CTA is mostly determined by the orientation of acetyl groups, the positive out-of-plane birefringence is attributed to the in-plane alignment of acetyl groups induced by solution casting, as reported in our previous paper [21]. The addition of LMCs greatly enhances the out-of-plane birefringence of CTA. The enhancement is caused by the orientation of LMC molecules in the film plane accompanied with CTA chains. In other words, the long axis of 5CB and the disk plane of TCP and TPP orient in the film plane.

[Fig.3]

205 **3.2. Optical Anisotropy of Stretched Films**

206 Figure 4 shows the wavelength dispersion of the in-plane and out-of-plane
207 birefringences of the CTA films stretched at a draw ratio of 1.5. The stretching temperatures
208 at which the tensile storage modulus is 10 MPa at a frequency of 10 Hz of pure CTA, and
209 CTA/TCP, CTA/TPP and CTA/5CB blends, were 214, 185, 184 and 188 °C, respectively.
210 Figure 4a reveals that CTA shows negative in-plane birefringence that decreases with
211 increasing wavelength, *i.e.*, ordinary wavelength dispersion, similar to most conventional
212 polymers [7,17,18,20]. The negative orientation birefringence of the CTA film indicates that
213 the direction of the polarizability anisotropy associated with the acetyl groups is
214 perpendicular to the main chain, which aligns in the stretching direction. Consequently, the
215 refractive index in the oriented direction is lower than that in the perpendicular direction, *i.e.*,
216 negative orientation birefringence, as reported previously [7,15-17,21,31]. After hot
217 stretching, both the in-plane and out-of-plane birefringences of CTA become negative (Figure
218 4b). This is reasonable because the acetyl groups are oriented perpendicular to the stretching
219 axis.

220 [Fig.4]

221 In contrast, the blends show anomalous behavior. The addition of 5CB markedly
222 increases both in-plane and out-of-plane birefringences and changes their sign from negative
223 to positive. The results obtained for stretched CTA/5CB correspond to the trends of the
224 solution-cast film in Figure 3. This is presumably caused by the large polarizability
225 anisotropy of 5CB with positive birefringence. The experimental results indicate that the 5CB
226 molecules are forced to orient in the stretching direction accompanying the alignment of the
227 polymer chains because of their nematic interaction [32-34]. It is known that a nematic
228 interaction occurs in a miscible system when an LMC molecule is of appropriate size to move

229 cooperatively with chain segments of a host polymer [35-38]. Besides the large polarizability
230 anisotropy, the strong nematic interaction between CTA and 5CB will also be responsible for
231 the pronounced orientation birefringence of this blend film. Upon addition of disk-shaped
232 LMCs, the sign of in-plane and out-of-plane birefringences changes from negative to positive
233 with extraordinary wavelength dispersion. Moreover, the enhancement of out-of-plane
234 birefringence is larger than that of in-plane birefringence.

235 The relationship between in-plane and out-of-plane birefringences of general
236 polymers after uniaxial stretching can be given by the following equation assuming uniaxial
237 symmetry deformation; *i.e.*, $n_y = n_z$ in equation (3).

238 $$\Delta n_{th} = \frac{\Delta n_{in}}{2} \qquad (4)$$

239 The birefringences of CTA seem to follow equation (4), as shown in Figure 4.
240 However, the difference in the out-of-plane birefringence between CTA and the blends with
241 LMCs is similar to that in the in-plane birefringence. In particular, the marked enhancement
242 of the out-of-plane birefringence induced by the disk-shaped LMCs compared with that of the
243 in-plane birefringence should be noted. These results are quite different from equation (4),
244 even considering the nematic interactions in the blend films. To clarify the mechanism of the
245 marked out-of-plane birefringence of the blend films, the interaction between CTA and the
246 LMCs was also evaluated by ATR measurements focusing on the C-O-C stretching vibration
247 in the pyranose ring (1029 cm^{-1}) and C=O stretching vibration in the carbonyl group (1735
248 cm^{-1}) (data not shown). None of the LMCs affect the position or intensity of the peaks from
249 the pyranose ring and carbonyl group of CTA, indicating that there is no specific interaction
250 such as chemical or electrostatic interactions between CTA and these LMCs.

To clarify the orientation of CTA chains in the blends, the drawn samples were immersed in methanol for 24 h to remove the LMCs following the method developed by Manaf *et al*. [16]. The orientation birefringence of the films was then measured again after drying at room temperature under vacuum.

[Fig.5]

After immersion in methanol for 24 h, there were no considerable changes in the dimensions of the samples, suggesting that the degree of stretching is hardly affected by methanol immersion. FT-IR spectra confirmed that all LMCs in the blend films were dissolved in the methanol during immersion.

The wavelength dispersion of the in-plane and out-of-plane birefringences of the stretched films after methanol immersion is presented in Figure 5. The birefringences of the blends decrease and approach to those of pure CTA following methanol immersion. This result demonstrates that the molecular orientation of CTA chains is not affected by LMC addition. This is reasonable because stretching of all films was performed at the same stress level as mentioned later. Furthermore, it is found from 2D-WAXD patterns that the intensity on the equator for (500) plane in the crystalline form of CTA-I is not affected by LMC addition, supporting the result in Figure 4.

The normalized refractive indices, *i.e.*, $n_i/\overline{n}$, along the three principal axes were calculated from both in-plane and out-of-plane birefringences and are depicted in Figure 6.

In the case of pure CTA, the normalized refractive indices in the *y* and *z* directions, *i.e.*, $n_y/\overline{n}$ and $n_z/\overline{n}$, are almost the same. However, n_y is slightly larger than n_z, suggesting that the CTA film shows transversal stretching to some degree. In other words, the transversal shrinkage in the film plane is smaller than the shrinkage in the thickness direction.

Consequently, the molecules are slightly oriented to the *y*-direction besides their marked orientation in the *x*-direction. This is reasonable because CTA will show pronounced strain-hardening during hot stretching because of the presence of crystallites [1,3]. As a result, planar elongational deformation, which is a kind of biaxial deformation, occurs rather than purely uniaxial deformation, especially in the center part of the film. This is observed in T-die film processing for a polymer with long-chain branches [22-25].

[Fig.6]

The stress-strain curves measured during hot stretching are shown in Figure 7. Both strain and stress are true values, assuming that the Poisson ratio is 0.5. The true stress increases monotonically with true strain. Because the final stress level is almost the same for all films, the degree of the orientation of CTA chains is the same, as discussed above (see Figure 5). Instead of quantitative evaluation of the strain-hardening, the width of the stretched films was measured. This information directly relates to the level of neck-in; that is, lateral reduction of the films. It is found that the width of the stretched films is almost the same as that of the initial unstretched films (reduction of just 5% compared with the initial film) at a draw ratio of 1.5. This result demonstrates that planar deformation occurs during uniaxial stretching in these experiments.

[Fig.6]

The refractive index anisotropy caused by planar deformation is magnified by LMC addition. In the case of rod-shaped molecules such as 5CB, however, the principal axis of the molecules is basically oriented in the *x*-direction. Therefore, the transversal (*y*-axis) orientation is not pronounced so much ($n_x >> n_y >> n_z$), because the long axis of 5CB has to change its direction to show the transversal orientation. On the contrary, disk-shaped

297 molecules tend to embed themselves in the film plane even for the low level of transversal
298 orientation of the polymer chains, because the transversal orientation does not disturb the *x*-
299 axis orientation of the disk-shaped LMC molecules. As a result, the blends show a larger
300 refractive index in the *y*-direction than that in the *z*-direction ($n_y >> n_z$). Furthermore, the
301 contribution of CTA chains ($n_y > n_x$) to the orientation birefringence is not negligible, so n_y is
302 larger than n_x.

303 Consequently, it can be concluded that the order of the refractive indices of the films
304 is as follows:

305 CTA,

306 $$n_y \geq n_z > n_x \quad (5)$$

307 CTA with disk-shaped LMC,

308 $$n_y > n_x > n_z \quad (6)$$

309 CTA with rod-shaped LMC,

310 $$n_x >> n_y >> n_z . \quad (7)$$

311 These experimental results demonstrates that the 3D control of refractive indices can
312 be achieved using an appropriate LMC only by uniaxial stretching, which has not been
313 reported to the best of our knowledge. The shape of LMC molecules is an important factor
314 influencing the refractive index ellipsoid of a stretched film. Furthermore, the crystallinity of
315 the film and stretching conditions will also affect the refractive index ellipsoid because they
316 determine the lateral orientation in the film plane. Finally, it is indicated that this technique
317 will be available for most polymer materials showing marked strain-hardening behavior in

elongational viscosity, in which polymers having a low degree of crystallinity with high T_m, such as poly(vinyl chloride) and poly(ethylene terephthalate) are included. Moreover, various methods have been proposed recently to provide the strain-hardening.[26-29] Therefore, advanced optical films will be prepared by uniaxial stretching in near future.

4. Conclusion

Uniaxial hot stretching of CTA, which contains a small amount of crystallites at the stretching temperature, causes transversal stretching in the film plane to some degree besides elongation in the stretching direction. This is directly confirmed by the change in dimensions of the film after hot stretching. Consequently, the orientation in the transversal direction is more pronounced than that in the thickness direction, leading to large out-of-plane birefringence compared with that for pure uniaxial deformation. The orientation birefringence caused by non-uniaxial deformation is greatly magnified by LMC addition, and can be controlled by the shape of the LMC molecules. In the case of disk-shaped molecules, both n_x and n_y are enhanced. Conversely, n_x is strongly enhanced with a slight increase in n_y by the addition of rod-shaped molecules. These experimental results suggest the great possibility of 3D control of refractive indices by adjusting the amount of crystallites in the matrix polymer and/or the shape of LMCs. Because an expensive biaxial stretching machine is not required at this technique, the industrial application will be considered seriously.

Acknowledgements

Financial support from the Thailand Research Fund through the Royal Golden Jubilee Ph.D. Program (Grant No. PHD/0099/2554) to Kultida Songsurang is gratefully acknowledged.

References

1. Edgar KJ, Buchanan CM, Debenham JS, Rundquist PA, Seiler BD, Shelton MC, Tindall D. Advances in cellulose ester performance and application. Prog Polym Sci 2001;26:1605-88.
2. Sairam M, Sreedhar B, Mohan Rao DV, Palaniappan S. Synthesis and thermal degradation kinetics of cellulose esters. Polym Adv Technol 2003;14:477-85.
3. Pulp Production and Processing: From Papermaking to High-Tech Products; Popa VI. Ed.; Smithers Rapra: Shawbury, 2013.
4. Müller F, Leuschke Ch. In Engineering Thermoplastics; Ch.5, Organic Cellulose Esters, Bottenbruch L. Ed.; Hanser: Munich, 1996.
5. Hahn BR, Wendorff JH. Compensation method for zero birefringence in oriented polymers. Polymer 1985;26:1619-22.
6. Tagaya A, Ohkita H, Harada T, Ishibashi K, Koike Y. Zero-birefringence optical polymers. Macromolecules 2006;39:3019-23.
7. Yamaguchi M, Manaf MEA, Songsurang K, Nobukawa S. Material design of retardation films with extraordinary wavelength dispersion of orientation birefringence - A review. Cellulose 2012;19:601-13.

8. Van Horn BL, Winter HH. Conoscopic measurement of birefringence and orientation in biaxially stretched polymer films and sheets. Macromolecules 2003;36:8513-21.
9. Yucel O, Unsal E, Cakmak M. Temporal Evolution of Optical Gradients during Drying in Cast Polymer Solutions. Macromolecules 2013;46:7112-7.
10. Eguchi Y, Unsal E, Cakmak M. Critical Phenomenon During Drying of Semiaromatic, Transparent and Soluble Polyimide Cast Films: Real-Time Observation of Birefringence and Other Integrated Parameters. Macromolecules 2013;46:7488-501.
11. Unsal E, Cakmak M. Real-Time Characterization of Physical Changes in Polyimide Film Formation: From Casting to Imidization. Macromolecules 2013;46:8616-27.
12. Uchiyama A, Yatabe T. Analysis of extraordinary birefringence dispersion of uniaxially oriented poly(2,6-dimethyl 1,4-phenylene oxide)/atactic polystyrene blend films. Jpn J Appl Phys 2003;42:3503-7.
13. Uchiyama A, Yatabe T. Control of birefringence dispersion of uniaxially oriented poly(2,6-dimethyl 1,4-phenylene oxide)/atactic polystyrene blend films by changing the stretching parameters. Jpn J Appl Phys 2003;42:5665-9.
14. Kuboyama K, Kuroda T, Ougizawa T. Control of wavelength dispersion of birefringence by miscible polymer blends. Macomol Symp 2007;249-250:641-6.
15. Yamaguchi M, Okada K, Manaf MEA, Shiroyama Y, Iwasaki T, Okamoto K. Extraordinary wavelength dispersion of orientation birefringence for cellulose esters. Macromolecules 2009;42:9034-40.
16. Manaf MEA, Tsuji M, Shiroyama Y, Yamaguchi M. Wavelength dispersion of orientation birefringence for cellulose esters containing tricresyl phosphate. Macromolecules 2011;44:3942-9.
17. Yamaguchi M, Iwasaki T, Okada K, Okamoto K. Control of optical anisotropy of cellulose esters and their blends with plasticizer. Acta Mater 2009;57:823-9.

387 18. Uchiyama A, Yatabe T. Control of wavelength dispersion of birefringence for oriented
388 copolycarbonate films containing positive and negative birefringent units. Jpn J Appl
389 Phys 2003;42:6941-5.
390 19. Koike Y, Yamazaki K, Ohkita H, Tagaya A. Zero-birefringence optical polymer by
391 birefringent crystal and analysis of the compensation mechanism. Macomol Symp
392 2006;235:64-70.
393 20. Yamaguchi M, Lee S, Manaf MEA, Tsuji M, Yokohara T. Modification of orientation
394 birefringence of cellulose ester by addition of poly(lactic acid). Eur Polym J
395 2010;46:2269-74.
396 21. Songsurang K, Miyagawa A, Manaf MEA, Phulkerd P, Nobukawa S, Yamaguchi M.
397 Optical anisotropy in solution-cast film of cellulose triacetate. Cellulose 2013;20:83-96.
398 22. Debroth T, Erwin L. Causes of edge beads in cast films. Polym Eng Sci 1986;26:462-7.
399 23. Satoh N, Tomiyama H, Kajiwara T. Viscoelastic simulation of film casting process for a
400 polymer melt. Polym Eng Sci 2001;41:1564-79.
401 24. Canning K, Co A. Edge effects in film casting of molten polymers. J Plast Film Sheet
402 2000;16:188-203.
403 25. Kouda S. Prediction of processability at extrusion coating for low-density polyethylene.
404 Polym Eng Sci 2008;48:1094-102.
405 26. Yamaguchi M, Miyata H. Strain hardening behavior in elongational viscosity for binary
406 blends of linear polymer and crosslinked polymer. Polym J 2000;32:164-71.
407 27. Yamane H, Sakai K, Takano M, Takahashi M. Poly(D-lactic acid) as a rheological
408 modifier of poly(L-lactic acid): shear and biaxial extensional flow behavior. J Rheol
409 2004;48:599-609.
410 28. Yokohara T, Nobukawa S, Yamaguchi M. Rheological properties of polymer composites
411 with flexible fine fiber. J Rheol 2011;55,1205-18.

412 29. Siriprumpoonthum M, Nobukawa S, Satoh Y, Sasaki H, Yamaguchi M. Effect of thermal
413 modification on rheological properties of polyethylene blends. J Rheol 2014;58:449-65.
414 30. Manaf MEA, Tsuji M, Nobukawa S, Yamaguchi M. Effect of moisture on the orientation
415 birefringence of cellulose esters. Polymers 2011;3:955-66.
416 31. Ferry JD. Viscoelastic Properties of Polymers, 3rd Ed., Wiley: New York, 1980.
417 32. Doi M, Watanabe H. Effect of nematic interaction on the Rouse dynamics.
418 Macromolecules 1991;24:740-44.
419 33. Watanabe H, Kotaka T, Tirrell M. Effect of orientation coupling due to nematic
420 interaction on relaxation of Rouse chains. Macromolecules 1991;24:201-8.
421 34. Zawada AF, Fuller GG, Colby RH, Fetters LJ, Roovers J. Measuring component
422 contributions to the dynamic modulus in miscible polymer blends. Macromolecules
423 1994;27:6851-60.
424 35. Urakawa O, Ohta E, Hori H, Adachi K. Effect of molecular size on cooperative
425 dynamics of low mass compounds in polystyrene. J Polym Sci Polym Phys Ed
426 2006;44:967-74.
427 36. Nobukawa S, Urakawa O, Shikata T, Inoue T. Evaluation of nematic interaction
428 parameter between polymer segments and low-mass molecules in the mixture.
429 Macromolecules 2010;43:6099-105.
430 37. Nobukawa S, Urakawa O, Shikata T, Inoue T. Cooperative dynamics in polystyrene and
431 low-mass molecule mixtures. Macromolecules 2011;44:8324-32.
432 38. Nobukawa S, Aoki Y, Yoshimura H, Tachikawa Y, Yamaguchi M. Effect of aromatic
433 additives with various alkyl groups on orientation birefringence of cellulose acetate
434 propionate. J Appl Polym Sci 2013;130:3465-72.
435 39. Yamaguchi M. Flow instability in capillary extrusion of plasticized poly(vinyl chloride).
436 J Appl Polym Sci 2001;82:1277-83.

40. Yamaguchi M, Wakabayashi T. Rheological properties and processability of chemically modified poly(ethylene terephthalate-co-ethylene isophthalate). Adv Polym Technol 2006;25:236-41.

440 **Figure Captions**

441 **Figure 1.** Chemical structure of LMC samples used in this study.

442 **Figure 2.** Temperature dependence of tensile storage modulus *E'* and loss tangent *tan* δ of
443 CTA (circles), CTA/TCP (95/5) (diamonds), CTA/TPP (95/5) (triangles) and
444 CTA/5CB (95/5) (squares) at 10 Hz.

445 **Figure 3.** Wavelength dispersion of the out-of-plane birefringence $\Delta n_{th}(\lambda)$ of solution-cast
446 films of CTA (circles), CTA/TCP (95/5) (diamonds), CTA/TPP (95/5)
447 (triangles) and CTA/5CB (95/5) (squares).

448 **Figure 4.** Wavelength dispersion of (a) in-plane birefringence $\Delta n_{in}(\lambda)$ and (b) out-of-
449 plane birefringence $\Delta n_{th}(\lambda)$ of stretched films of CTA (circles), CTA/TCP
450 (95/5) (diamonds), CTA/TPP (95/5) (triangles) and CTA/5CB (95/5) (squares).
451 The draw ratio was 1.5.

452 **Figure 5.** Wavelength dispersion of (a) in-plane birefringence $\Delta n_{in}(\lambda)$ and (b) out-of-
453 plane birefringence $\Delta n_{th}(\lambda)$ of stretched films of CTA (circles), CTA/TCP
454 (95/5) (diamonds) and CTA/TPP (95/5) (triangles) after immersion in methanol.
455 The draw ratio was 1.5.

456 **Figure 6.** Wavelength dispersion of normalized refractive indices along the three principal
457 axes of CTA, CTA/TCP, CTA/TPP and CTA/5CB films.

458 **Figure 7.** True stress (σ_T) – true strain (ε_T) curves of films of CTA (circles), CTA/TCP
459 (95/5) (diamonds), CTA/TPP (95/5) (triangles) and CTA/5CB (95/5) (squares).

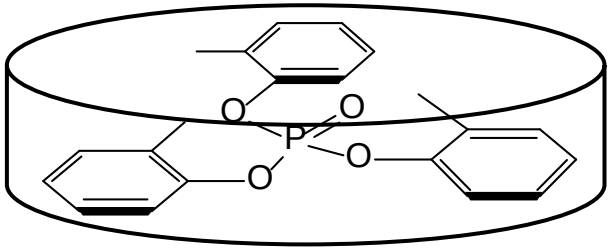

TCP

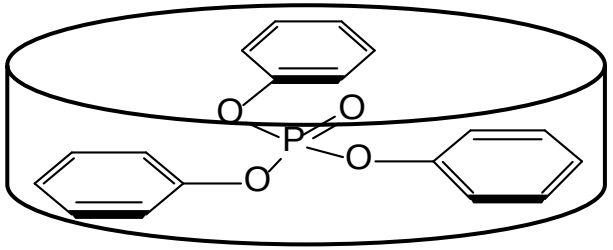

TPP

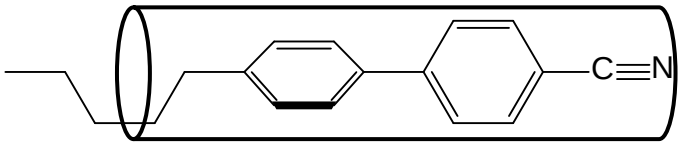

5CB

Songsurang et al., Figure 1

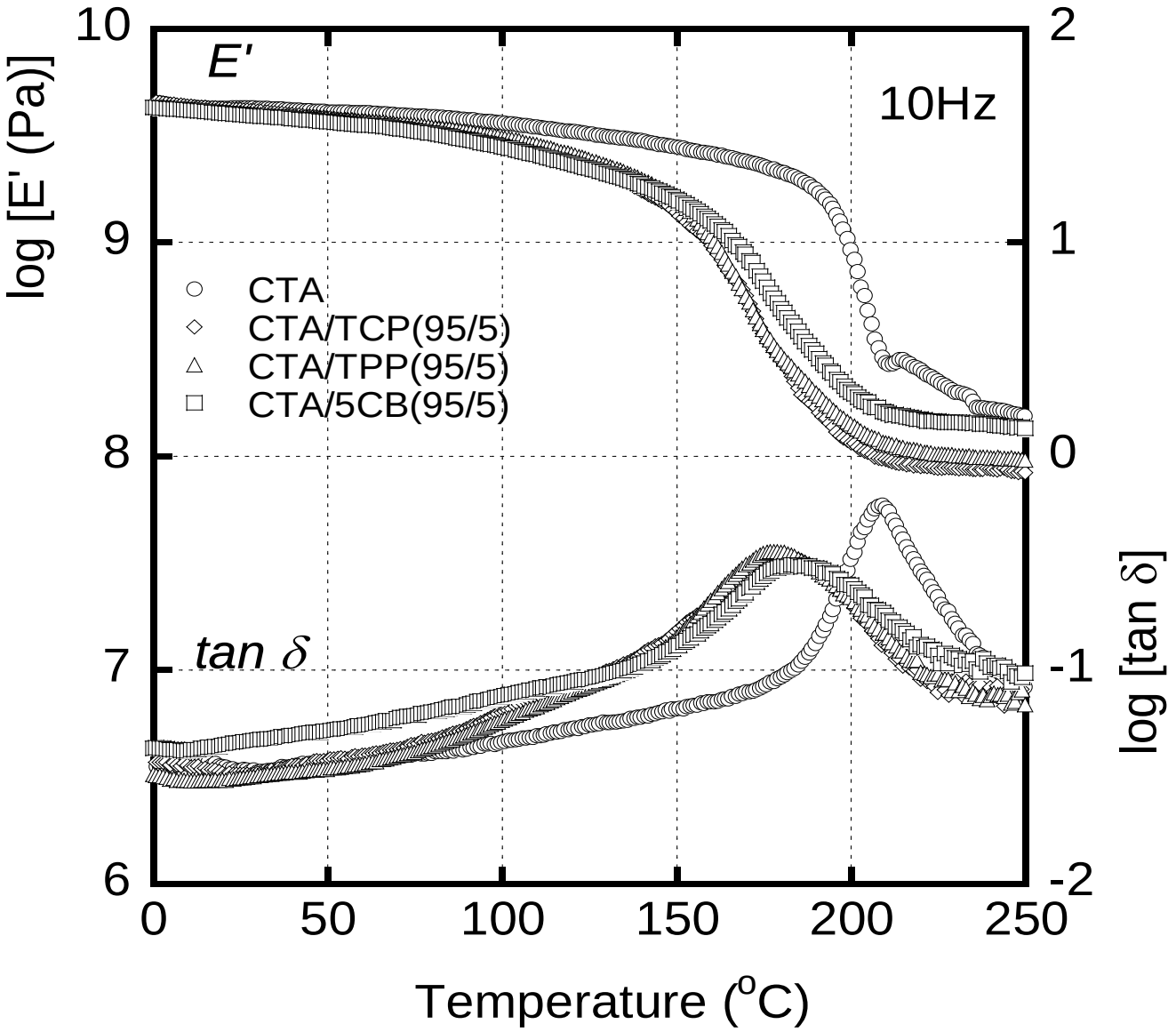

Songsurang et al., Figure 2

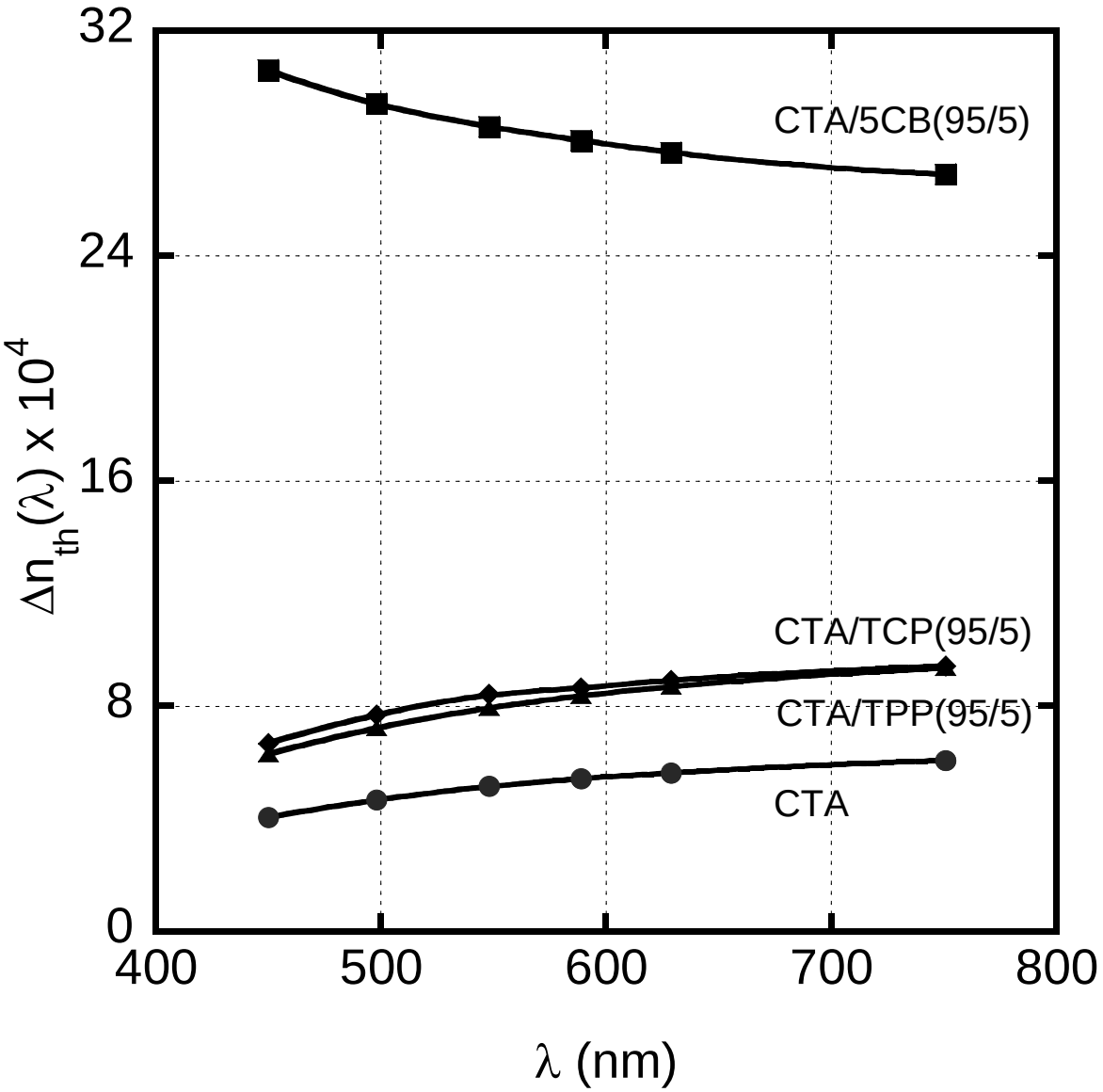

Songsurang et al., Figure 3

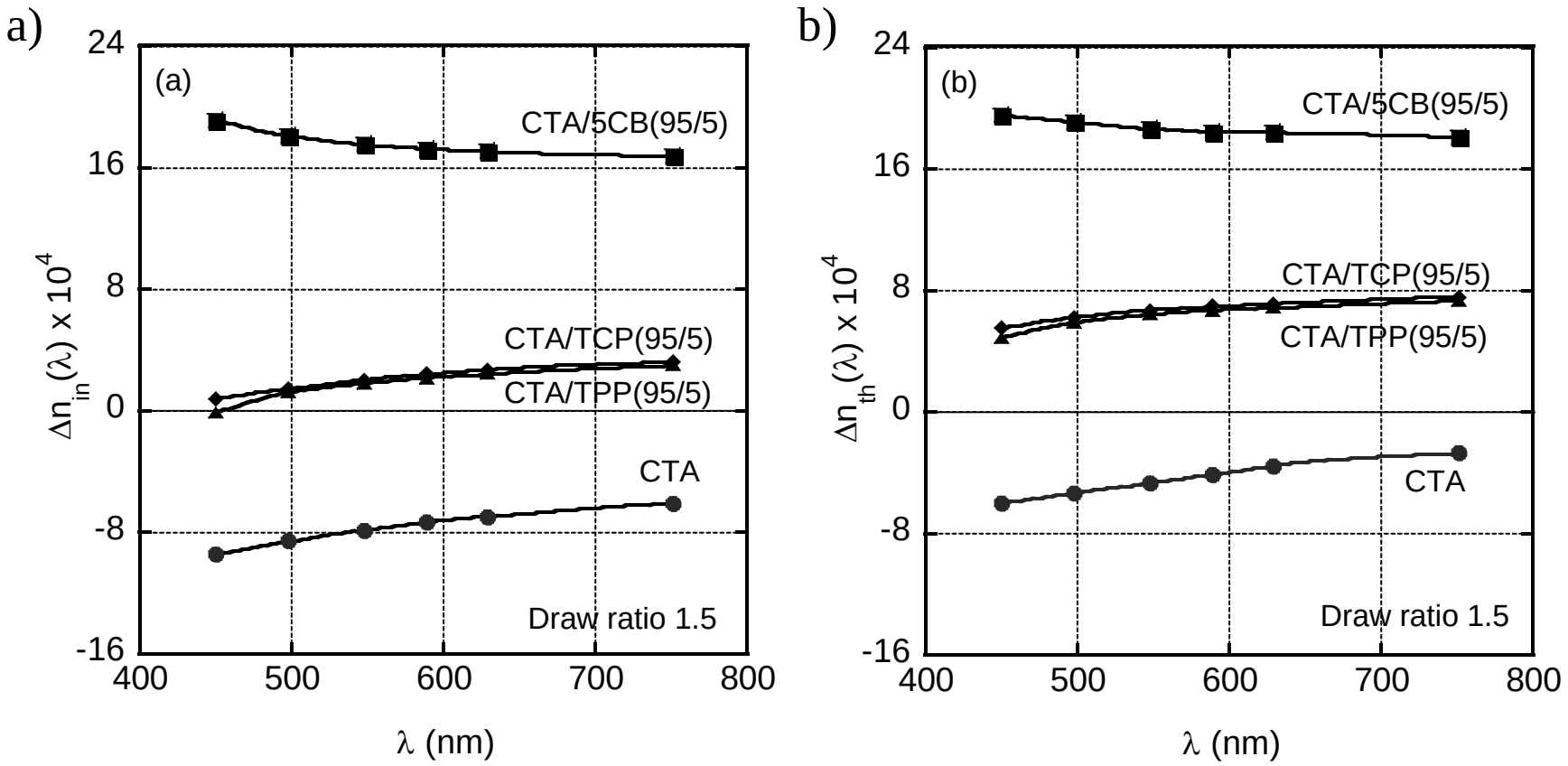

Songsurang et al., Figure 4

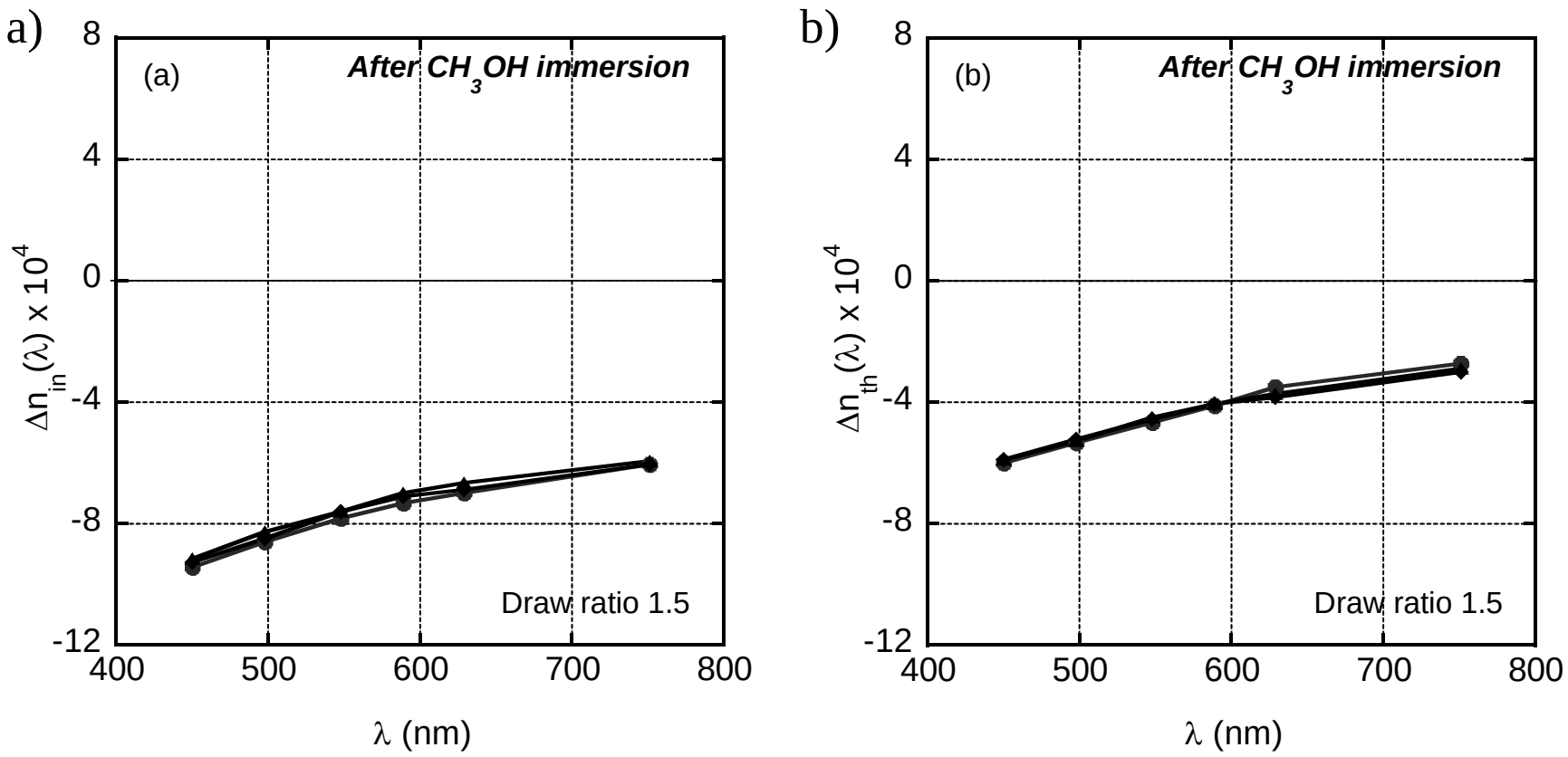

Songsurang et al., Figure 5

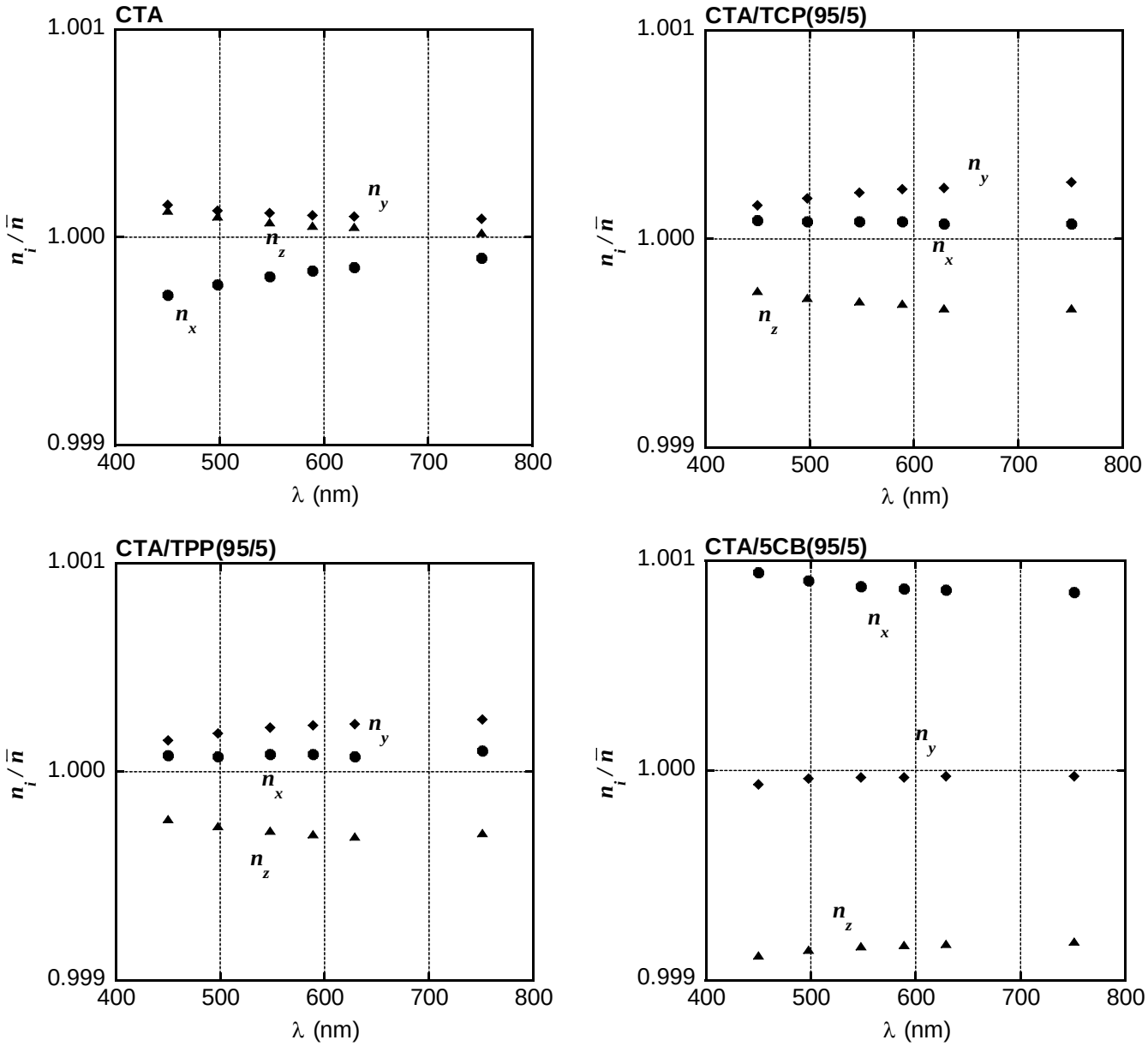

Songsurang et al., Figure 6

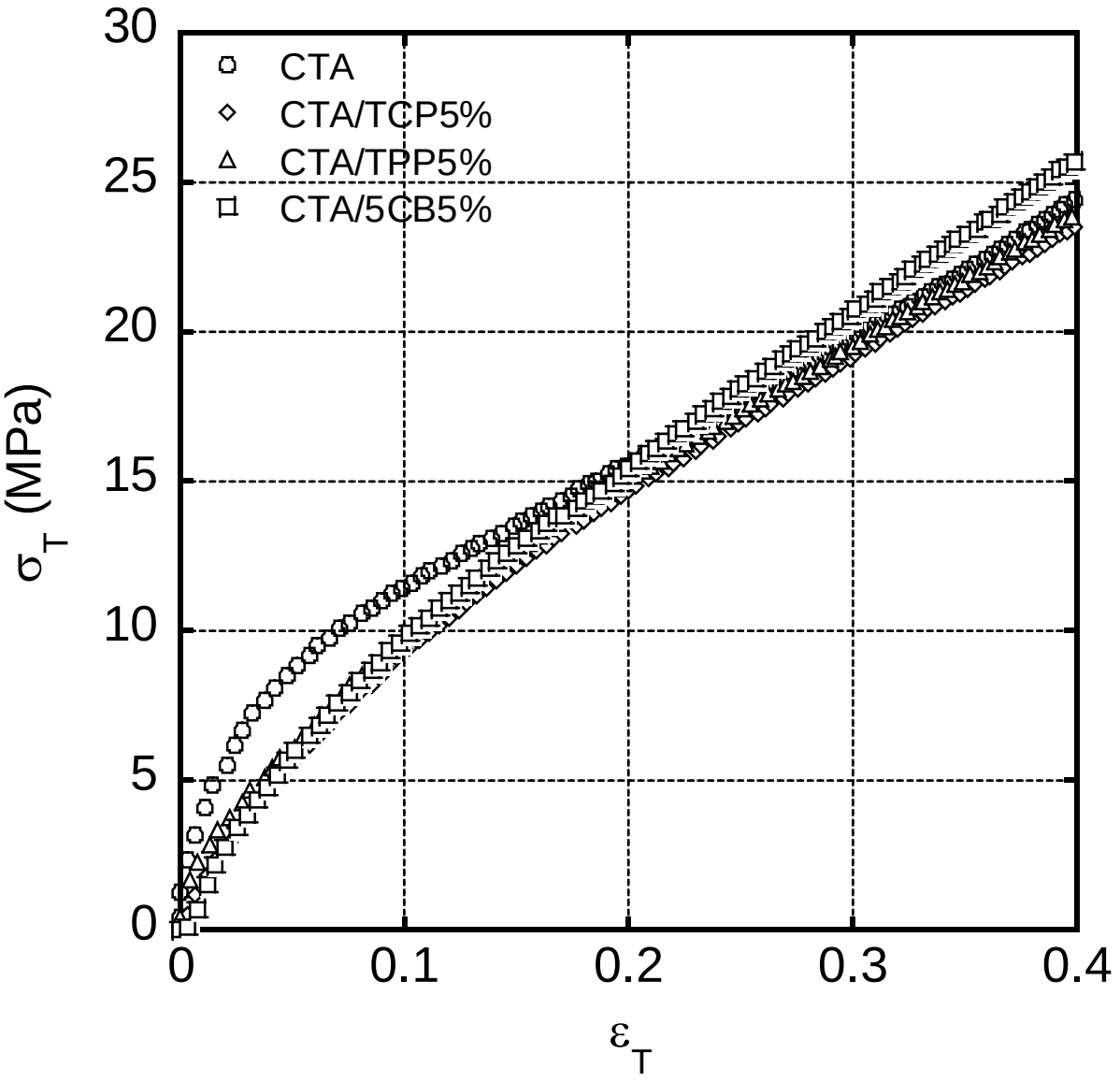

Songsurang et al., Figure 7

Disk-shaped LMC

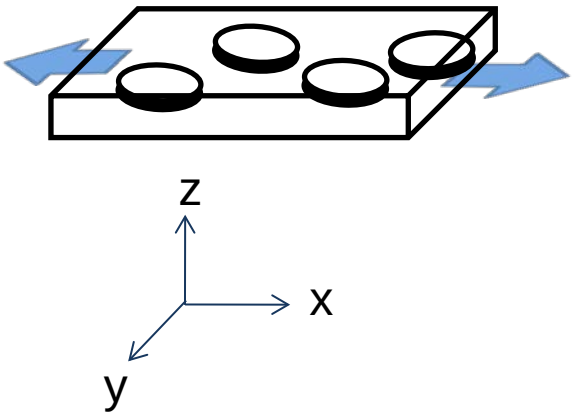

Rod-shaped LMC

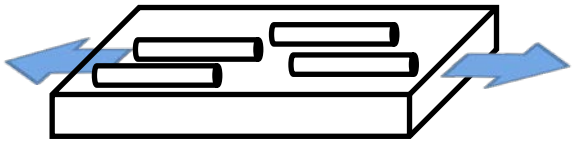

	Top-View (x, y)	Side-View (x, z)	Effect of LMC addition		
			n_x	n_y	n_z
Disk-shaped LMC	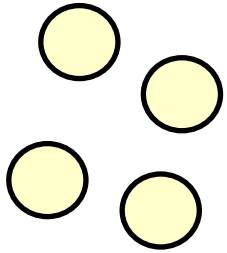	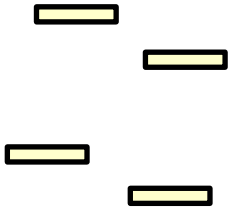	++	++	a little
Rod-shaped LMC	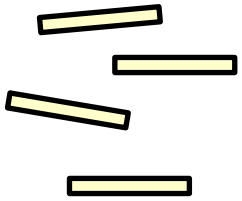	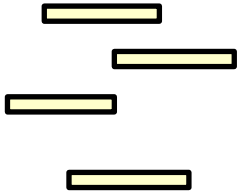	+++	+	a little

x: stretching direction
y: transversal direction
z: thickness direction